

# Discontinuous Galerkin Methods For One And Two Dimensional Schrödinger Equations

Ömer Aktepe

## 1 Introduction

In this study, we consider 2 dimensional Schrödinger equations,

$$iu_t + \Delta u - vu = 0, \quad x \in \Omega, t > 0,$$

where  $\Omega$  is an interval or a square,  $u$  is a complex wave function,  $i = \sqrt{-1}$  is the imaginary unit,  $\Delta$  is the Laplace operator, and  $v$  is a real smooth potential function with either  $v = f(|u|^2)$  for an arbitrary smooth real function  $f$  or  $v = v(x)$ . We also assume periodic boundary conditions.

Many numerical methods are developed to solve Schrödinger equations, and due to its high order Galerkin methods are one of those. First studies [8, 9, 10, 11, 12] solve nonlinear time-dependent hyperbolic equations with high order Runge-Kutta methods. Recently, there are a couple of new papers on discontinuous Galerkin method. For example, [3] focuses on repeatedly applying integration by parts so all the spatial derivatives are shifted from the solution to the test function in the weak formulations, and [4] is about linear first-order transport equations and two-way wave equations. In [13] the authors presented a LDG method with exponential time differencing Runge-Kutta scheme, and investigated the energy conservation performance of the scheme. [2] gives several conservative and stable numerical schemes to approximate the coupled nonlinear Schrödinger equations where the schemes are uniquely solvable and convergent. More recently, in studies [5] and [6] authors use mass preserving discontinuous Galerkin schemes for NLS. The direct discontinuous Galerkin method is applied to Schrödinger equation in [6] which includes alternating fluxes, and energy conservation and optimal accuracy are achieved. In this study, we look at [1] which follows [6] in time discretization Crank-Nicolson method is used for linear Schrödinger equation and the Strang splitting method is used for nonlinear Schrödinger case.

## 1.1 Derivation of Schrödinger equation

We will derive the equation from the wave mechanics. For this purpose, we will first assume

$$\psi(x, t) = A e^{i(kx - \omega t)}$$

and introduce a couple of formulas from physics. We know the following formulas related to energy from physics:

$$\begin{aligned} E &= T + V = \frac{p^2}{2m} + V(x) \\ E &= \hbar\omega \\ k &= \frac{p}{\hbar} \end{aligned}$$

where  $E$ ,  $T$  and  $V$  represents total, kinetic and potential energy respectively,  $\hbar$  is the reduced Plank constant and  $p$  is the momentum. We multiply the first equation by  $\psi$  and obtain

$$\begin{aligned} E\psi &= \frac{p^2}{2m}\psi + V(x)\psi \\ \hbar\omega\psi &= \frac{p^2}{2m}\psi + V(x)\psi \end{aligned}$$

Now we look at partial derivatives of  $\psi$

$$\begin{aligned} \frac{\partial\psi}{\partial t} &= -i\omega\psi \\ \frac{\partial^2\psi}{\partial x^2} &= -k^2\psi = -\frac{p^2}{\hbar^2}\psi \end{aligned}$$

and replace the previous equation by these terms to obtain

$$i\hbar\frac{\partial\psi}{\partial t} = -\frac{\hbar^2}{2m}\frac{\partial^2\psi}{\partial x^2} + V\psi$$

## 1.2 Discontinuous Galerkin Method

The discontinuous Galerkin method is a finite element method that projects the solution into a finite dimensional space while using test functions from the very same space. In our study, we choose this space to be spanned by completely discontinuous piecewise polynomials.

The first time discontinuous Galerkin method was in 1973 by Reed and Hill [16] in a time independent linear hyperbolic equation. Since then, the method is used various studies and equations, such as, electrodynamics, fluid mechanics and plasma physics.

Due to totally discontinuous basis functions, the discontinuous Galerkin method provides various advantages such as,

- Any order of accuracy can be achieved, and this can be done in each cell separately.
- It can be used on any complicated spatial domain and boundary condition with arbitrary triangulation.
- Progression of the solution during time in each cell depends entirely on surrounding cells.
- For any scalar equation and order of accuracy in any domain and any triangulation, there is a provable cell entropy and  $L^2$  stability according to [17].
- $(k + \frac{1}{2})$ -th order of accuracy is guaranteed and in fact for smooth solutions it is often  $(k + 1)$  when piecewise polynomials of degree  $k$  are used.

Now, we will demonstrate essential ideas of the discontinuous Galerkin method on an one dimensional heat equation

$$u_t - u_{xx} = 0 \quad (1)$$

for  $x \in [0, 2\pi]$  with initial condition  $u(x, 0) = \sin(x)$  and with periodic boundary condition. We denote  $I_j = [x_{j-\frac{1}{2}}, x_{j+\frac{1}{2}}]$  for  $j = 1, \dots, N$  as a mesh for spacial domain where  $x_{\frac{1}{2}} = 0$  and  $x_{N+\frac{1}{2}} = 2\pi$ . For simplicity, we consider uniform mesh with mesh size  $h$ . We denote the center of each cell  $I_j$  by  $x_j$  and width of each cell by  $h = x_{j+\frac{1}{2}} - x_{j-\frac{1}{2}}$ .

We multiply (1) by any test function  $\nu$  which vanishes outside of the interval  $I_j$ , integrate over  $I_j$  and apply integration by parts to get

$$\int_{I_j} u_t \nu dx + \int_{I_j} u_x \nu_x dx - u_x(x_{j+\frac{1}{2}}, t) \nu(x_{j+\frac{1}{2}}) + u_x(x_{j-\frac{1}{2}}, t) \nu(x_{j-\frac{1}{2}}) = 0. \quad (2)$$

For discontinuous Galerkin method, we define the approximation space and the test function space as

$$V_h = \{\nu : \nu(x) \text{ is a piecewise polynomial of degree at most } k \text{ on } I_j, j = 1, \dots, N\}$$

and consider  $u$  and  $\nu$  to be in  $V_h$ . Since the approximation space consists of piecewise discontinuous functions,  $u$  and  $\nu$  are not well defined on boundary of each cell, and so are constants in (2).

The discontinuous Galerkin method suggests replacing constants in (2), and there are various ways to do this. [18] and [19] suggest modifying (2) by

$$\begin{aligned} & \int_{I_j} u_t \nu dx + \int_{I_j} u_x \nu_x dx - (\hat{u}_x)_{j+\frac{1}{2}} \nu_{j+\frac{1}{2}}^- + (\hat{u}_x)_{j-\frac{1}{2}} \nu_{j-\frac{1}{2}}^+ \\ & - \frac{1}{2} (\nu_x)_{j+\frac{1}{2}}^- (u_{j+\frac{1}{2}}^+ - u_{j+\frac{1}{2}}^-) - \frac{1}{2} (\nu_x)_{j-\frac{1}{2}}^+ (u_{j-\frac{1}{2}}^+ - u_{j-\frac{1}{2}}^-) = 0 \end{aligned} \quad (3)$$

where  $\nu_{j+\frac{1}{2}}^-$ ,  $\nu_{j-\frac{1}{2}}^+$ ,  $(\nu_x)_{j+\frac{1}{2}}^-$ ,  $u_{j+\frac{1}{2}}^+$ ,  $u_{j+\frac{1}{2}}^-$ ,  $(\nu_x)_{j-\frac{1}{2}}^+$ ,  $u_{j-\frac{1}{2}}^+$  and  $u_{j-\frac{1}{2}}^-$  represent values defined inside of  $I_j$ , and central fluxes are defined as

$$(\hat{u}_x)_{j+\frac{1}{2}} = \frac{1}{2} \left( (u_x)_{j+\frac{1}{2}}^- + (u_x)_{j+\frac{1}{2}}^+ \right) \quad (4)$$

$$(\hat{u}_x)_{j-\frac{1}{2}} = \frac{1}{2} \left( (u_x)_{j-\frac{1}{2}}^- + (u_x)_{j-\frac{1}{2}}^+ \right) \quad (5)$$

We can rewrite (3) in a more global and compact way:

$$\int_0^{2\pi} u_t \nu dx + \sum_{j=1}^N \left( \int_{I_j} u_x \nu_x dx + (\hat{u}_x)_{j+\frac{1}{2}} [\nu]_{j+\frac{1}{2}} - (\hat{\nu}_x)_{j-\frac{1}{2}} [u]_{j-\frac{1}{2}} \right) \quad (6)$$

where the jump function at the interface is defined as  $[w] = w^+ - w^-$ , and the central flux is defined as  $(\hat{\nu}_x)_{j+\frac{1}{2}} = \frac{1}{2} \left( (\nu_x)_{j+\frac{1}{2}}^- + (\nu_x)_{j+\frac{1}{2}}^+ \right)$ .

## 2 One Dimensional Schrödinger equation

We consider one dimensional nonlinear Schrödinger equations of the form,

$$iu_t + u_{xx} + fu = 0, \quad x \in \mathbb{R}, t > 0,$$

where  $u$  is a complex wave function, and  $f$  is either  $f = f(x)$  or  $f = f(|u^2|)$ , where  $f(u)$  is a nonlinear real function. We will assume that  $u$  is periodic, and restrict  $x$  to an interval  $[a, b]$  by letting  $u(a) = u(b)$ .

### 2.1 One Dimensional Discontinuous Galerkin Method

For one dimensional discontinuous Galerkin method, take the interval  $[a, b]$ , and define

$$a = x_{1/2} < x_{3/2} < \cdots < x_{N+1/2} = b,$$

$$I_j = [x_{j-1/2} + x_{j+1/2}], \quad x_j = \frac{1}{2}(x_{j-1/2} + x_{j+1/2}) \quad \text{and}$$

$$h_j = x_{j+1/2} - x_{j-1/2} \quad h = \max_j h_j.$$

We define the approximation space  $V_h^k = \{\nu : \nu|_{I_j} \in P^k(I_j), j = 1, \dots, N\}$  where  $P^k(I_j)$  are polynomials centered at  $x_j$  up to degree  $k$ . Given any  $\nu \in P^k(I_j)$  we can multiply the equation by  $\nu$ , and take integral over  $x$ . For any  $t > 0$ , we have

$$i \int_{I_j} \nu u_t dx + \int_{I_j} \nu u_{xx} dx + \int_{I_j} \nu f(|u|^2) u dx = 0. \quad (7)$$

On  $I_j$  we can let  $u(x, t) \simeq u_h(x, t) = \sum_{m=0}^k \varphi_m(t) p_m(x)$  for any  $t > 0$  and  $p_l \in P^k(I_j)$ . Then (7) becomes a system of nonlinear ode's

$$\sum_{m=0}^k \left( i \int_{I_j} \nu \varphi'_m(t) p_m(x) dx + \int_{I_j} \nu \varphi_m(t) p''_m(x) dx + \int_{I_j} \nu f(|u_h|^2) \varphi_m(t) p_m(x) dx \right) = 0 \quad (8)$$

We modify (8) by applying integration by parts two times at (7) to the second integral. If we do this, we get:

$$\begin{aligned} i \int_{I_j} \nu u_t dx + \int_{I_j} \nu_{xx} u dx + \int_{I_j} \nu f(|u|) u dx \\ + \nu u_x|_{x_{j-1/2}}^{x_{j+1/2}} - \nu_x u|_{x_{j-1/2}}^{x_{j+1/2}} = 0. \end{aligned} \quad (9)$$

At points  $x_j$ ,  $u_h$  has different left and right values depending on the interval. So, we need modification for the constant terms in (9). Lets define jump and average for  $u_h$  by

$$[u_h] = u_h^+ - u_h^- \quad \text{and} \quad \{u_h\} = \frac{1}{2}(u_h^+ + u_h^-)$$

respectively. Here note that as  $u$  is periodic for  $j = 1$  and  $j = N$  these definitions are still well defined. Now, we say

$$\begin{aligned}\nu_x u_h|_{x_{j-1/2}}^{x_{j+1/2}} &\simeq \nu_x \hat{u}_h|_{x_{j-1/2}}^{x_{j+1/2}} \\ \nu(u_h)_x|_{x_{j-1/2}}^{x_{j+1/2}} &\simeq \nu(\tilde{u}_h)_x|_{x_{j-1/2}}^{x_{j+1/2}}\end{aligned}$$

where we define

$$\begin{aligned}(\tilde{u}_h)_x &= \{(u_h)_x\} + \alpha_1[(u_h)_x] + \beta_1[u_h] \quad \text{and} \\ \hat{u}_h &= \{u_h\} + \alpha_2[u_h] + \beta_2[(u_h)_x] \quad \alpha_{1,2}, \beta_{1,2} \in \mathbb{C}.\end{aligned}$$

So, for any  $j \in \{1, \dots, N\}$  (9) becomes

$$\begin{aligned}i \int_{I_j} \nu(u_h)_t dx + \int_{I_j} \nu_{xx} u_h dx + \int_{I_j} \nu f(|u_h|^2) u_h dx \\ + \nu(\tilde{u}_h)_x|_{x_{j+1/2}} - \nu(\tilde{u}_h)_x|_{x_{j-1/2}} - \nu_x \hat{u}_h|_{x_{j+1/2}} + \nu_x \hat{u}_h|_{x_{j-1/2}} = 0.\end{aligned}\quad (10)$$

We can write this on any  $I_j$  as

$$\begin{aligned}\sum_{m=0}^k i\varphi'_m(t) \int_{I_j} \nu p_m dx + \sum_{m=0}^k \varphi_m(t) \int_{I_j} \nu'' p_m dx + \sum_{m=0}^k \varphi_m(t) \int_{I_j} \nu f(|u_h|^2) p_m dx \\ + \nu(\tilde{u}_h)_x|_{x_{j+1/2}} - \nu(\tilde{u}_h)_x|_{x_{j-1/2}} - \nu_x \hat{u}_h|_{x_{j+1/2}} + \nu_x \hat{u}_h|_{x_{j-1/2}} = 0.\end{aligned}\quad (11)$$

In order see the whole system, lets redefine: for all  $t \geq 0$

$$\begin{aligned}u_h(x, t) &= \sum_{m=0}^k \varphi_{j,m}(t) p_{j,m}(x) \quad \text{on } I_j \\ \nu &= p_{j,l} \quad \text{on } I_j\end{aligned}$$

Then the equation (11) becomes

$$\begin{aligned}\sum_{m=0}^k i\varphi'_{j,m}(t) \int_{I_j} p_l p_m dx + \sum_{m=0}^k \varphi_{j,m}(t) \int_{I_j} p_l'' p_m dx + \sum_{m=0}^k \varphi_{j,m}(t) \int_{I_j} f(|u_h|^2) p_l p_m dx \\ + (p_{j,l}(\tilde{u}_h)_x|_{x_{j+1/2}} - p_{j,l}(\tilde{u}_h)_x|_{x_{j-1/2}} - (p_{j,l})_x \hat{u}_h|_{x_{j+1/2}} + (p_{j,l})_x \hat{u}_h|_{x_{j-1/2}}) = 0.\end{aligned}\quad (12)$$

where

$$\begin{aligned}
p_{j,l}(\tilde{u}_h)_x|_{x_{j+1/2}} &= (p_{j,l} \sum_{m=0}^k (\frac{1}{2} + \alpha_1)p'_{j+1,m}\varphi_{j+1,m} + (\frac{1}{2} - \alpha_1)p'_{j,m}\varphi_{j,m} \\
&\quad + \beta_1 p_{j+1,m}\varphi_{j+1,m} - \beta_1 p_{j,m}\varphi_{j,m})|_{x_{j+1/2}} \\
p_{j,l}(\tilde{u}_h)_x|_{x_{j-1/2}} &= (p_{j,l} \sum_{m=0}^k (\frac{1}{2} + \alpha_1)p'_{j,m}\varphi_{j,m} + (\frac{1}{2} - \alpha_1)p'_{j-1,m}\varphi_{j-1,m} \\
&\quad + \beta_1 p_{j,m}\varphi_{j,m} - \beta_1 p_{j-1,m}\varphi_{j-1,m})|_{x_{j-1/2}} \\
(p_{j,l})_x \hat{u}_h|_{x_{j+1/2}} &= (p'_{j,l} \sum_{m=0}^k (\frac{1}{2} + \alpha_2)p_{j+1,m}\varphi_{j+1,m} + (\frac{1}{2} - \alpha_2)p_{j,m}\varphi_{j,m} \\
&\quad + \beta_2 p'_{j+1,m}\varphi_{j+1,m} - \beta_2 p'_{j,m}\varphi_{j,m})|_{x_{j+1/2}} \\
(p_{j,l})_x \hat{u}_h|_{x_{j-1/2}} &= (p'_{j,l} \sum_{m=0}^k (\frac{1}{2} + \alpha_2)p_{j,m}\varphi_{j,m} + (\frac{1}{2} - \alpha_2)p_{j-1,m}\varphi_{j-1,m} \\
&\quad + \beta_2 p'_{j,m}\varphi_{j,m} - \beta_2 p'_{j-1,m}\varphi_{j-1,m})|_{x_{j-1/2}}
\end{aligned}$$

So, we obtained a system of nonlinear ode's with  $(k+1)N$  many equations and unknowns:

$$A\varphi' + G\varphi + F(\varphi) = 0 \quad (13)$$

where  $\varphi, A, G$  and  $F(\varphi)$  are of the form

$$\varphi = ([\varphi_{1,0}, \varphi_{1,1}, \dots, \varphi_{1,k}], \dots, [\varphi_{j,0}, \varphi_{j,1}, \dots, \varphi_{j,k}], \dots, [\varphi_{N,0}, \varphi_{N,1}, \dots, \varphi_{N,k}])^t$$

$$\begin{aligned}
A &= \begin{pmatrix} A_1 & & & \\ & \ddots & & \\ & & A_j & \\ & & & \ddots & A_N \end{pmatrix} \text{ for } (A_j)_{l,m} = i \int_{I_j} p_l p_m dx, \\
G &= \begin{pmatrix} G_{1,1} & G_{1,2} & & & G_{1,N} \\ & \ddots & & & \\ & & G_{j,j-1} & G_{j,j} & G_{j,j+1} \\ & & & \ddots & \\ & & & & G_{N,N-1} & G_N \end{pmatrix} \text{ for} \\
(G_{j,j})_{l,m} &= \int_{I_j} p_l'' p_m dx + (p_{j,l}((\frac{1}{2} - \alpha_1)p'_{j,m} - \beta_1 p_{j,m}))|_{x_{j+1/2}} + (p_{j,l}((\frac{1}{2} + \alpha_1)p'_{j,m} + \beta_1 p_{j,m}))|_{x_{j-1/2}} \\
&\quad + (p'_{j,l}((\frac{1}{2} - \alpha_2)p_{j,m} - \beta_2 p'_{j,m}))|_{x_{j+1/2}} + (p'_{j,l}((\frac{1}{2} + \alpha_2)p_{j,m} + \beta_2 p'_{j,m}))|_{x_{j-1/2}} \\
(G_{j,j-1})_{l,m} &= (p_{j,l}((\frac{1}{2} - \alpha_1)p'_{j-1,m} - \beta_1 p_{j-1,m}))|_{x_{j-1/2}} + (p'_{j,l}((\frac{1}{2} - \alpha_2)p_{j-1,m} - \beta_2 p'_{j-1,m}))|_{x_{j-1/2}} \\
(G_{j,j+1})_{l,m} &= (p_{j,l}((\frac{1}{2} + \alpha_1)p'_{j+1,m} + \beta_1 p_{j+1,m}))|_{x_{j+1/2}} + (p'_{j,l}((\frac{1}{2} + \alpha_2)p_{j+1,m} + \beta_2 p'_{j+1,m}))|_{x_{j+1/2}} \\
\text{and } F(\varphi) &= \begin{pmatrix} \hat{f}(\varphi_{1,.}) & & & \\ & \ddots & & \\ & & \hat{f}(\varphi_{j,.}) & \\ & & & \ddots & \hat{f}(\varphi_{1N,.}) \end{pmatrix} \\
\text{for } (\hat{f}(\varphi_{j,.}))_{l,m} &= \int_{I_j} f(|\sum_{n=0}^k \varphi_{j,n} p_{j,n}|^2) p_l p_m dx.
\end{aligned}$$

## 2.2 Implicit-Explicit Runge-Kutta Method

Consider the ode system  $u' = f(u) + g(u)$  where  $f$  corresponds to a convection (hyperbolic) term (in our case it is nonlinear part of the equation) and  $g$  corresponds to a diffusion (parabolic) term (in our case it is the diffusion part of the equation). We consider an  $(s+1)$ -stage and  $s$ -stage DIRK schemes [14] of the form

$$\begin{array}{c|ccccccccc}
0 & 0 & 0 & 0 & \cdots & 0 & 0 & 0 & 0 & \cdots & 0 \\
c_1 & 0 & a_{1,1} & 0 & \cdots & 0 & c_1 & \hat{a}_{2,1} & 0 & 0 & \cdots & 0 \\
c_2 & 0 & a_{2,1} & a_{2,2} & \cdots & 0 & c_2 & \hat{a}_{3,1} & \hat{a}_{3,2} & 0 & \cdots & 0 \\
\vdots & \vdots & \vdots & \vdots & \ddots & 0 & \vdots & \vdots & \vdots & \vdots & \ddots & 0 \\
c_s & 0 & a_{s,1} & a_{s,2} & \cdots & a_{s,s} & c_{s-1} & \hat{a}_{s,1} & \hat{a}_{s,2} & \hat{a}_{s,3} & \cdots & 0 \\
\hline
& 0 & b_1 & b_2 & \cdots & b_s & & \hat{b}_1 & \hat{b}_2 & \hat{b}_3 & \cdots & \hat{b}_s
\end{array}$$

and

IMEX scheme [7] from  $t_{n-1}$  to  $t_n = t_{n-1} + dt$  is given by following formulas:

$$u_n = u_{n-1} + dt \sum_{j=1}^s b_j K_j + dt \sum_{j=1}^{s+1} \hat{b}_j \hat{K}_j$$

where we set  $\hat{K}_1 = f(u_{n-1})$  and for  $i = 1, \dots, s$

$$\begin{aligned}
w_i &= u_{n-1} + dt \sum_{j=1}^i a_{i,j} K_j + dt \sum_{j=1}^i \hat{a}_{i,j} \hat{K}_j \quad \text{where } K_i = g(w_i) \\
\hat{K}_{i+1} &= f(w_i)
\end{aligned}$$

iteratively give  $K_j$ 's and  $\hat{K}_j$ 's. We consider two-stage third order DIRK schemes for the implicit( $s$ -stage) and the explicit( $s+1$ -stage) parts (respectively):

$$\begin{array}{c|cc}
\gamma & \gamma & 0 \\
\hline
1-\gamma & 1-2\gamma & \gamma \\
\hline
1/2 & 1/2
\end{array}
\quad \text{and} \quad
\begin{array}{c|ccc}
0 & 0 & 0 & 0 \\
\hline
\gamma & \gamma & 0 & 0 \\
\hline
1-\gamma & \gamma-1 & 2(1-\gamma) & 0 \\
\hline
0 & 1/2 & 1/2 & 1/2
\end{array}$$

for  $\gamma = (3 + \sqrt{3})/6$ .

To solve the system (13) we use third order IMEX Runge-Kutta method.

With appropriate choice of flux parameters  $\alpha_{1,2}, \beta_{1,2}$  the mass  $\int_I |u|^2 dx$  is preserved. The stability is guaranteed due to [5].

**Theorem:** (Stability) The solution of semi-discrete DG scheme (5) using numerical fluxes satisfy  $L^2$  stability condition

$$\frac{d}{dt} \int_I |u_h|^2 dx \leq 0$$

if  $\Im \beta_{1,2} \geq 0$  and  $|\alpha_1 + \bar{\alpha}_2|^2 \leq -4\Im \beta_1 \Im \beta_2$ . If all parameters are real and  $\alpha_1 + \alpha_2 = 0$ , then

$$\frac{d}{dt} \int_I |u_h|^2 dx = 0$$

with no restriction on  $\beta_{1,2}$ .

### 2.3 Numerical Results for one dimensional case

In the following example, we use "A third-order combination" Runge-Kutta method given in [7] for  $dt = 0.001$  and the final time  $T = 1$  in order to solve

(11). The errors are given in  $L^2$  norm at time  $T$  which is defined by

$$\|u - u_h\|_2 = \left( \int_{\Omega} |u(\cdot, T) - u_h(\cdot, T)|^2 dx dy \right)^{1/2}$$

and use uniform mesh with  $N \times N$  many square cells.

*Example:* For the equation  $iu_t + u_{xx} + |u|^2u + |u|^4u = 0$  where  $x \in [-\pi, \pi]$ , we have the exact solution  $u(x, t) = e^{i(x+t)}$ . We set the flux variables  $\alpha_{1,2}$  and  $\beta_{1,2}$  to 0 and obtained Table 1 and order of these errors are at Figure 1. In Figures 2 up to 12, the first row is real part of approximate solution, exact solution and their difference respectively while the second rows are imaginary parts and we took  $\Delta t = 0.001$ .  $N$  represents number of grid points, and  $P^k$  represents polynomials upto order  $k$ . The blank parts in the table are due to computational limitations of the computer that is used for solving the problem.

	$P^1$	$P^2$	$P^3$	$P^4$
$N = 10$	1.0860e-01	1.4043e-02	1.7450e-04	7.7739e-06
$N = 20$	2.3596e-02	3.4918e-03	8.3924e-06	2.4868e-07
$N = 40$	5.6991e-03	2.7313e-04	5.1032e-07	
$N = 80$	1.4150e-03	3.5129e-05	7.4506e-08	
$N = 160$	3.5311e-04	4.4042e-06		

Table 1: Errors for Example when using  $P^k$ ,  $k = 1, 3, 4$  polynomials on a uniform mesh of  $N \times N$  cells,  $\alpha_{1,2} = \beta_{1,2} = 0$ . Final time is  $T = 1$

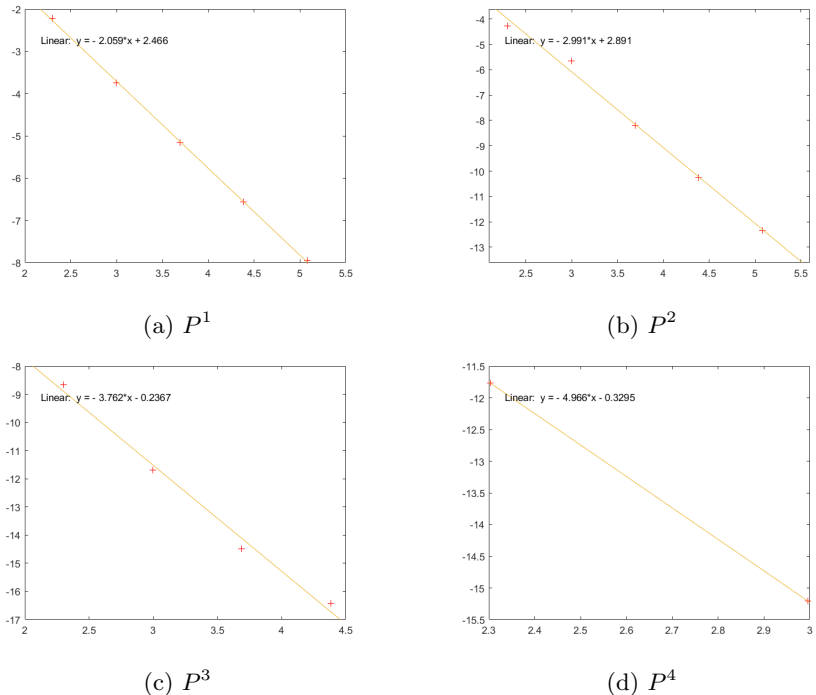


Figure 1: Order of errors for Table 1

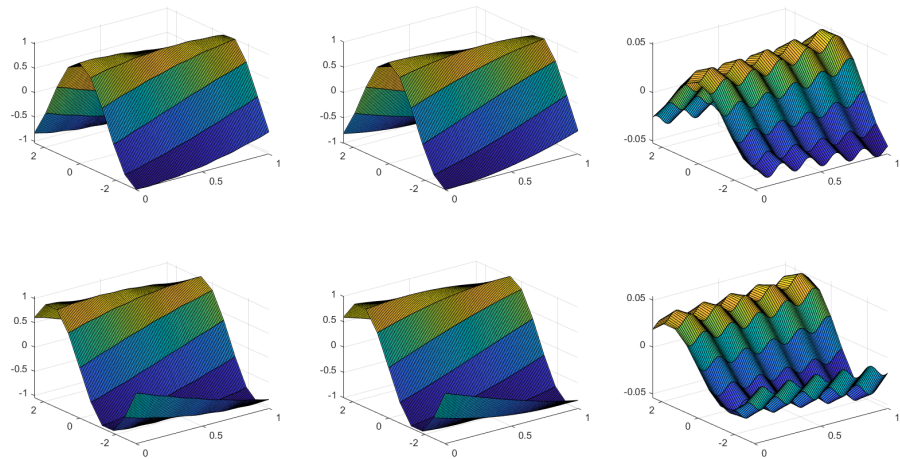


Figure 2: For  $\alpha_{1,2} = \beta_{1,2} = 0$ ,  $\Delta t = 0.01$ ,  $N = 10$  and  $P^1$

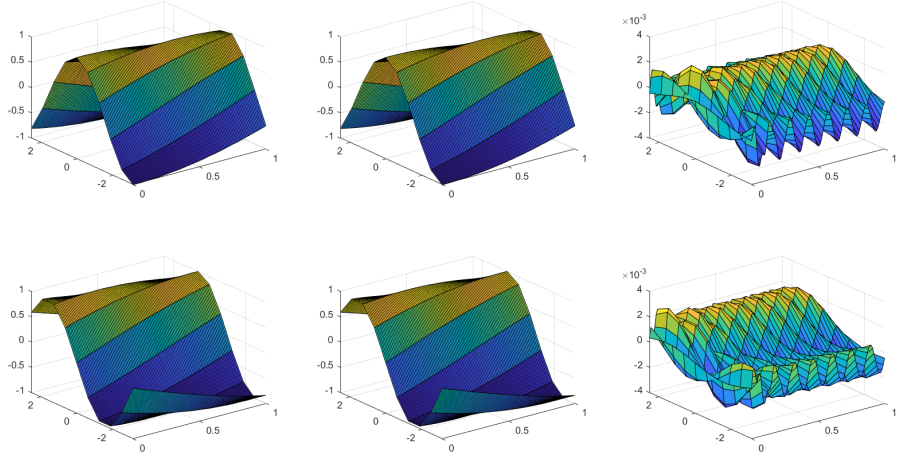


Figure 3: For  $\alpha_{1,2} = \beta_{1,2} = 0$ ,  $\Delta t = 0.01$ ,  $N = 10$  and  $P^2$

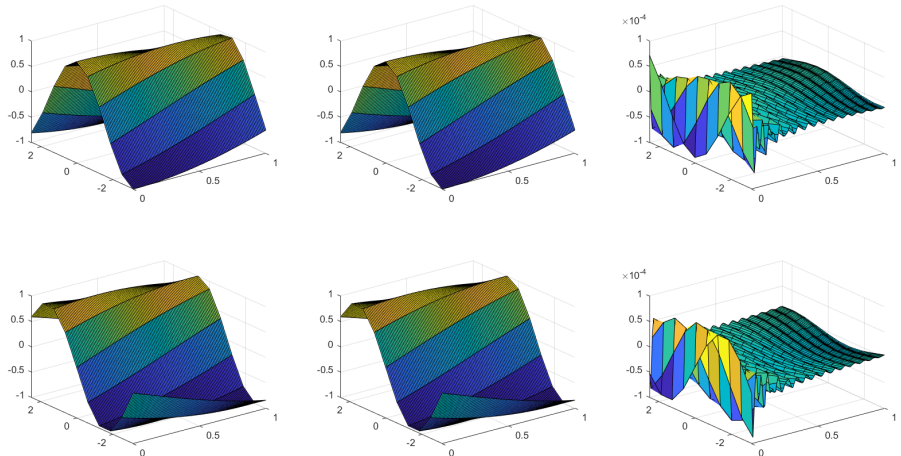


Figure 4: For  $\alpha_{1,2} = \beta_{1,2} = 0$ ,  $\Delta t = 0.01$ ,  $N = 10$  and  $P^3$

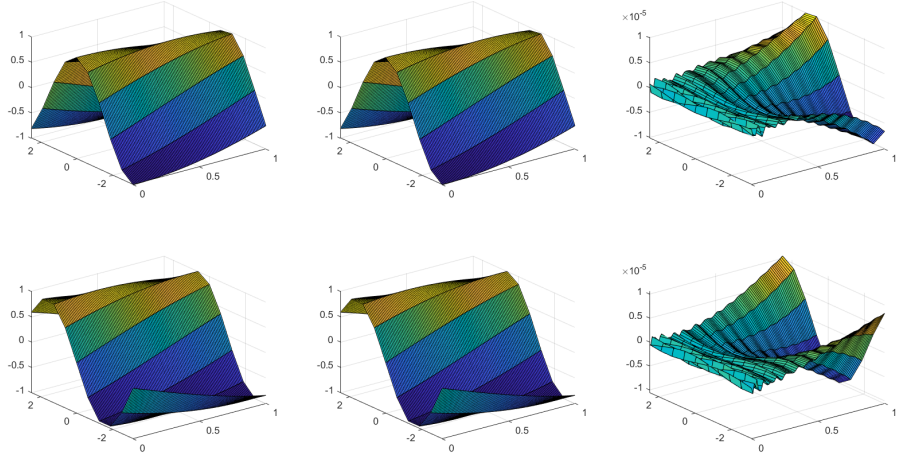


Figure 5: For  $\alpha_{1,2} = \beta_{1,2} = 0$ ,  $\Delta t = 0.01$ ,  $N = 10$  and  $P^4$

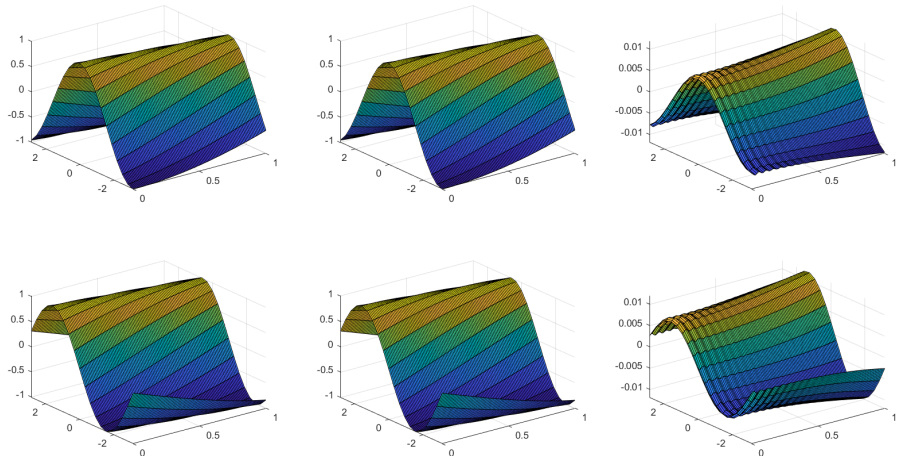


Figure 6: For  $\alpha_{1,2} = \beta_{1,2} = 0$ ,  $\Delta t = 0.01$ ,  $N = 20$  and  $P^1$

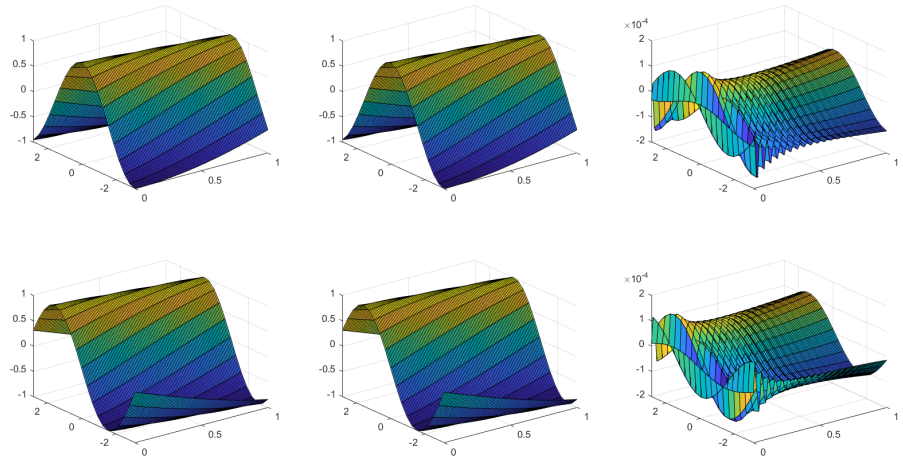


Figure 7: For  $\alpha_{1,2} = \beta_{1,2} = 0$ ,  $\Delta t = 0.01$ ,  $N = 20$  and  $P^2$

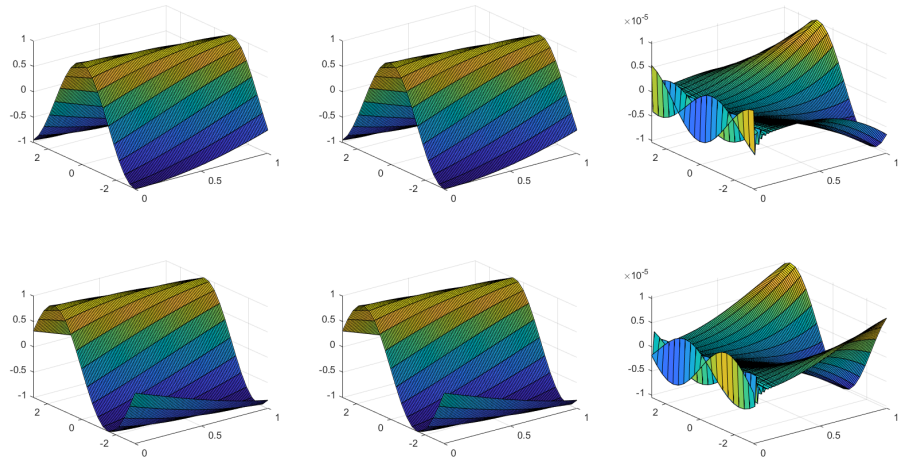


Figure 8: For  $\alpha_{1,2} = \beta_{1,2} = 0$ ,  $\Delta t = 0.01$ ,  $N = 20$  and  $P^3$

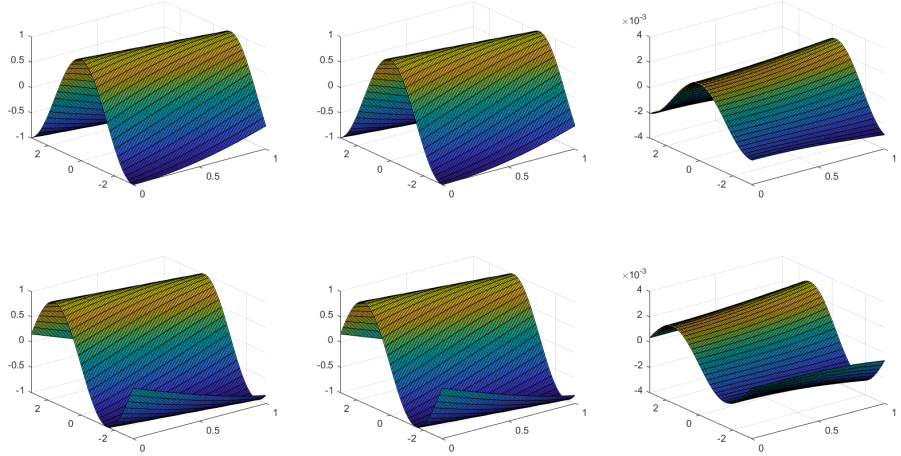


Figure 9: For  $\alpha_{1,2} = \beta_{1,2} = 0$ ,  $\Delta t = 0.01$ ,  $N = 40$  and  $P^1$

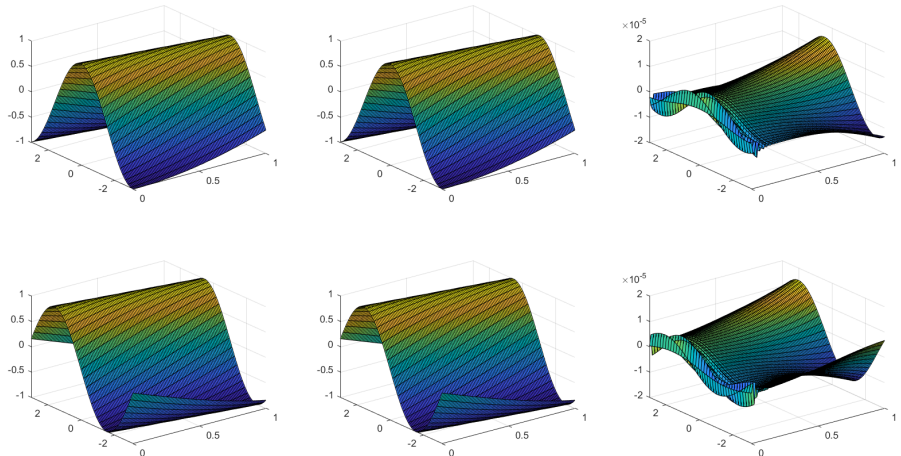


Figure 10: For  $\alpha_{1,2} = \beta_{1,2} = 0$ ,  $\Delta t = 0.01$ ,  $N = 40$  and  $P^2$

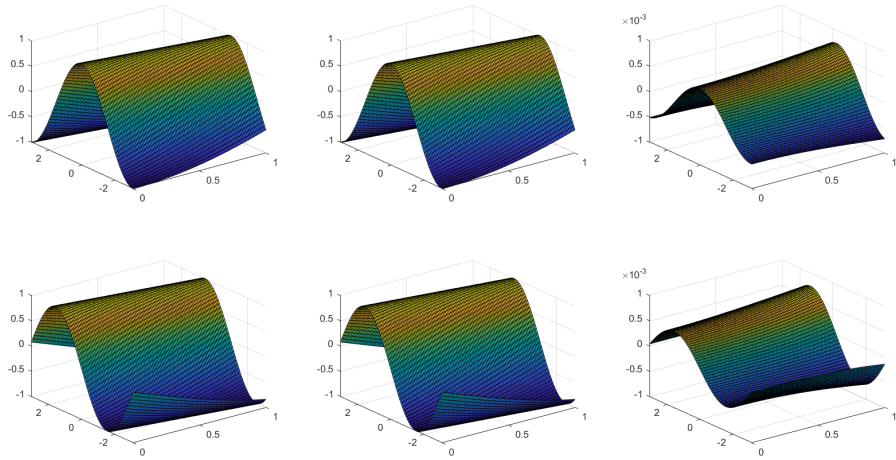


Figure 11: For  $\alpha_{1,2} = \beta_{1,2} = 0$ ,  $\Delta t = 0.01$ ,  $N = 80$  and  $P^1$

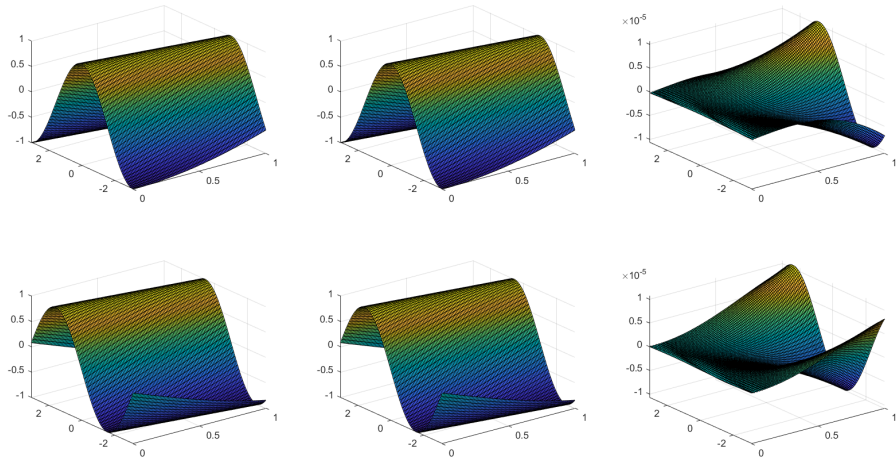


Figure 12: For  $\alpha_{1,2} = \beta_{1,2} = 0$ ,  $\Delta t = 0.01$ ,  $N = 80$  and  $P^2$

### 3 Two Dimensional Schrödinger equation

The equation can be written of the form:

$$\begin{aligned} i\psi_t + \Delta\psi - V\psi &= 0, \quad x \in \Omega, t > 0, \\ \psi(x, 0) &= \psi_0(x) \end{aligned} \tag{14}$$

where and  $\Omega \subset \mathbb{R}^2$ ,  $\psi$  is the complex wave function describing the state of elementary particle and  $V$  is a smooth and real function. We identify the equation depending on  $V$ . If  $V = 0$ , then it is called linear Schrödinger equation, if  $V = V(|\psi|^2)$ , then it is called nonlinear Schrödinger equation, and if  $V = V(x)$ , then it is called generalized nonlinear Schrödinger equation.

#### 3.1 Two Dimensional Discontinuous Galerkin Method

We take a finite partition  $\{\Omega_j\}$  of the domain  $\Omega$ . On each  $\Omega_j$  define the approximation space

$$V_h = \{\nu : \nu \in P^k(\Omega_j), \forall j\}$$

where  $P^k(\Omega_j)$  is the space spanned by all polynomials of degree  $k$  or less, and approximate  $\psi$  on  $\Omega_j$  by

$$\psi_h = \sum_{n=1} a_n(t) p_n(x) \tag{15}$$

where  $p_n$ 's form a basis for the polynomial space  $P^k(\Omega_j)$  and  $a_n$ 's are unknowns. In this paper, we always consider  $\Omega_j$ 's as rectangles however the discontinuous Galerkin method does not require such an assumption. Then, we have  $\Omega = \cup_{\alpha=1}^N \Omega_\alpha$  where  $\alpha = (\alpha_1, \dots, \alpha_d)$ ,  $N = (N_1, \dots, N_d)$  with  $\Omega_\alpha = I_{\alpha_1}^1 \times \dots \times I_{\alpha_d}^d$  for  $I_{\alpha_i}^i = [x_{\alpha_i-1/2}^i, x_{\alpha_i+1/2}^i]$  and  $\alpha_i \in \{1, \dots, N_i\}$ . This detailed representation will come in handy when we investigate the convergence of our method. We let  $h$  to be the maximum edge in this set of rectangles  $\Omega_j$ 's. Also note that  $d = 2$  as we restrict the problem on  $\mathbb{R}^2$ .

Now, we multiply the Schrödinger equation by a test function  $\nu \in V_h(\Omega_j)$ , and integrate over the space variables

$$i \int_{\Omega_j} \psi_{h,t} \nu dx + \int_{\Omega_j} \Delta\psi_h \nu dx - \int_{\Omega_j} V\psi_h \nu dx = 0$$

We apply Green's equation to obtain

$$i \int_{\Omega_j} \psi_{h,t} \nu dx - \int_{\Omega_j} \nabla\psi_h \nabla\nu dx + \int_{\partial\Omega_j} \nu \partial_n \psi_h ds - \int_{\Omega_j} V\psi_h \nu dx = 0$$

where  $n$  is the outward normal vector of  $\Omega_j$ . Before we generalize this formula on  $\Omega$ , we see that  $\psi_h$  and  $\nu$  are double valued on each  $e \in \Gamma_h$ , which is the set

of boundaries of  $\Omega_j$ 's. So, for  $\nu \in V_h$  we consider the discontinuous Galerkin scheme:

$$i \int_{\Omega} \psi_{h,t} \nu dx = \sum_n \int_{\Omega_n} \nabla \psi_h \nabla \nu dx + \sum_{e \in \Gamma_h} \int_e ([\nu] \widehat{\partial_n \psi_h} + [\psi_h] \{\partial_n \nu\}) ds + \int_{\Omega} V \psi_h \nu dx \quad (16)$$

where we define

$$\begin{aligned} [w] &= w_2 - w_1 \\ \{w\} &= \frac{1}{2}(w_2 + w_1) \\ \widehat{\partial_n \psi_h} &= \beta h_e^{-1} [\psi_h] + \{\partial_n \psi_h\} \\ h_e &= |\overrightarrow{C_1 C_2} \cdot \vec{n}|. \end{aligned}$$

We consider two neighbor cells say,  $\Omega_1$  and  $\Omega_2$ , with a common edge  $e$ . By  $w_i$  we mean the representation of  $w$  on  $\Omega_i$  and by  $C_i$  we mean the center of the rectangle  $\Omega_i$  for  $i \in \{1, 2\}$ . If  $e \in \Gamma_h \cap \partial\Omega$ , then we take  $\vec{n}$  to be the outward normal vector to  $\partial\Omega \cap e$ . If  $e \in \Gamma_h \setminus \partial\Omega$ , then  $\vec{n}$  represents the unit normal vector from  $C_1$  to  $C_2$ . However, this orientation choice of  $\vec{n}$  is not important since we do not put any condition about how  $\Omega_1$  and  $\Omega_2$  should be positioned. In fact, if we open the line integral in (16), we see that (16) is independent of this choice. Finally, the parameter  $\beta \in \mathbb{R}$  will be selected in order to achieve optimal convergence.

Under these constraints we have the following theorem for the 2 dimensional case due to [1].

**Theorem:** Let  $\psi_h$  to be the solution to the scheme above with any  $\beta$  except for  $k(k + \cos(k + 1 + 2j/N)\pi)/2$  with  $j$  running from 0 to  $N_i - 1$  for each fixed  $i = 1, \dots, d$ , and  $u$  a smooth solution to the Schrödinger equation. Then we have the error estimate

$$\|\psi_h(\cdot, t) - \psi(\cdot, t)\| \leq Ch^{k+1}$$

where  $C$  depends on  $\|\psi\|_{k+2}$ ,  $\|\psi_t\|_{k+1}$ ,  $\|V\|_\infty$ ,  $T$  linearly and the data given, but is independent of  $h$ .

By this theorem we ensure the convergence of the solution  $\psi_h$  of (16) to the exact solution of the Schrödinger equation, and only thing left to do is solving ODE given by (16) where the unknowns are  $a_j$ 's given in (15).

If we let  $A = (a_1^1, a_2^1, \dots, a_l^1, \dots, a_i^j, \dots, a_l^M)$  where the upper index  $j$  represents the cell  $\Omega_j$  that  $a_i^j$  belongs, we have the systems

$$\begin{aligned} C \dot{A}(t) &= DA(t) \\ C \dot{A}(t) &= DA(t) + F\bar{V}(A(t)) \end{aligned}$$

where the first formula is for the linear case, and the second one is for the nonlinear case. Matrices  $C$ ,  $D$  and  $F$  are constant matrices coming from the integration in (16), and  $\bar{V}(A)$  is a nonlinear term depending on  $A$ , and coming from the nonlinear part of (16).

### 3.2 Crank-Nicolson and Strang Methods

Let  $\psi^n \in V_h$  be the given solution of (16) at time  $t_n$ , and we want to compute  $\psi^{n+1} \in V_h$  which is the solution at time  $t_{n+1}$ .

When  $V = V(x)$  we use Crank-Nicolson method to solve (16). For this purpose, we discretize (16) in time. We consider the fully discrete scheme

$$\begin{aligned} i \int_{\Omega} \frac{\psi^{n+\frac{1}{2}} - \psi^n}{\Delta t/2} \nu dx &= \sum_n \int_{\Omega_n} \nabla \psi^{n+\frac{1}{2}} \nabla \nu dx \\ &+ \sum_{e \in \Gamma_h} \int_e ([\nu] \widehat{\partial_n \psi^{n+\frac{1}{2}}} + [\psi^{n+\frac{1}{2}}] \{\partial_n \nu\}) ds + \int_{\Omega} V^{n+\frac{1}{2}} \psi^{n+\frac{1}{2}} \nu dx \end{aligned} \quad (17)$$

where  $V^{n+\frac{1}{2}} = V(x)$ , solve it for  $\psi^{n+\frac{1}{2}} \in V_h$  for all  $\nu \in V_h$ , and let  $\psi^{n+1} = 2\psi^{n+\frac{1}{2}} - \psi^n$ .

When  $V = f(|\psi|^2)$  we use Strang splitting method to solve (16). We split (14) into 2 steps:

$$i\psi_t = V\psi \quad (18)$$

$$i\psi_t = -\Delta\psi \quad (19)$$

For given solution  $u^n$  at time  $t_n$ , we follow the following algorithm:

- Solve (18) for half time by

$$\psi^* = \psi^n e^{-if(|\psi^n|^2)\Delta t/2} \quad (20)$$

- Solve (19) by Crank-Nicolson similarly described as above: find  $u \in V_h$  such that for all  $\nu \in V_h$

$$i \int_{\Omega} \frac{\psi - \psi^*}{\Delta t/2} \nu dx = \sum_n \int_{\Omega_n} \nabla \psi \nabla \nu dx + \sum_{e \in \Gamma_h} \int_e ([\nu] \widehat{\partial_n \psi} + [\psi] \{\partial_n \nu\}) ds \quad (21)$$

and let  $\psi^{**} = 2\psi - \psi^*$ .

- Solve (18) for half time by

$$\psi^{n+1} = \psi^{**} e^{-if(|\psi^{**}|^2)\Delta t/2} \quad (22)$$

and this is the solution of (14) at time  $t_{n+1}$ .

Here note that in case  $V = f(|\psi|^2) + g(x)$  where  $g$  is independent of  $\psi$  we replace (18) and (19) by

$$\begin{aligned} i\psi_t &= f(|\psi|^2)\psi \\ i\psi_t &= -\Delta\psi + g(x)\psi \end{aligned}$$

The only part we adjust at the algorithm above is (21), and we replace it by

$$i \int_{\Omega} \frac{\psi - \psi^*}{\Delta t/2} \nu dx = \sum_n \int_{\Omega_n} \nabla \psi \nabla \nu dx + \sum_{e \in \Gamma_h} \int_e ([\nu] \widehat{\partial_n \psi} + [\psi] \{\partial_n \nu\}) ds + \int_{\Omega} g^{n+\frac{1}{2}} \psi \nu dx$$

where  $g^{n+\frac{1}{2}} = g(x)$ .

### 3.3 Numerical Results for two dimensional case

We will solve the scheme (16) using the Crank-Nicolson method for the linear case and the Strang method for the nonlinear case and refer to [15] on preservation of the mass. In examples, we assume periodic boundary condition, and the errors are given in  $L^2$  norm at final time  $T = 1$  which is defined by

$$\|\psi - \psi_h\|_2 = \left( \int_{\Omega} |\psi(\cdot, T) - \psi_h(\cdot, T)|^2 dx dy \right)^{1/2}$$

and use uniform mesh with  $N \times N$  many square cells.

*Example 1:* We take the linear Schrödinger equation

$$iu_t + \Delta u = 0, \quad u(x, y, 0) = e^{-i(x+y)}, \quad (x, y) \in [0, 2\pi]^2, \quad t \geq 0,$$

with periodic boundary condition which has the exact solution

$$u(x, y, t) = e^{-i(x+y+2t)}.$$

In this example, we take the flux parameter to be  $\beta = 0, 5, 10, 15$ , and use polynomial space  $P^k$  for  $k = 1, 2, 3, 4$  on uniform mesh with  $N \times N$  rectangular cells where  $N = 10, 20, 30, 40$ . For time steps  $\Delta t = 0.001$ , we have the Table 2 when  $\beta = 0$ , the Table 3 when  $\beta = 5$ , the Table 4 when  $\beta = 10$  and the Table 5 when  $\beta = 15$ . The Table 4 seems to be the best option among others, and order of the errors in Table 4 are given in Figure 13. Blank parts in tables are due to computational limitations of the computer that is used for solving the problem.

	$P^1$	$P^2$	$P^3$	$P^4$
$N = 10$	3.04e-01 0.363166 sec	6.94e-02 0.496415 sec	5.20e-03 1.4343.2757 sec	4.02e-04 3.319176 sec
$N = 20$	6.09e-02 1.918282 sec	1.00e-02 7.955216 sec	3.28e-04 22.852428 sec	1.18e-05 55.270677 sec
$N = 30$	2.71e-02 9.943695 sec	3.61e-03 44.400332 sec	1.95e-04 142.284123 sec	
$N = 40$	1.55e-02 33.213912 sec	1.80e-03 163.338707 sec	5.18e-05 629.740250 sec	

Table 2: Errors for Example 1 when using  $P^k$ ,  $k = 1, 3, 4$  polynomials on a uniform mesh of  $N \times N$  cells,  $\beta = 0$ . Final time is  $T = 1$

	$P^1$	$P^2$	$P^3$	$P^4$
$N = 10$	1.8924 0.222186 sec	3.36e-02 0.492279 sec	3.23e-03 1.483285 sec	1.89e-04 3.824531 sec
$N = 20$	5.08e-01 2.188379 sec	3.53e-03 9.644957 sec	1.37e-04 25.146125 sec	8.74e-06 59.896196 sec
$N = 30$	2.28e-01 12.076300 sec	9.58e-04 45.755220 sec	2.64e-05 158.200532 sec	
$N = 40$	1.29e-01 41.053604 sec	4.04e-04 205.788439 sec	8.81e-06 643.807859 sec	

Table 3: Errors for Example 1 when using  $P^k$ ,  $k = 1, 3, 4$  polynomials on a uniform mesh of  $N \times N$  cells,  $\beta = 5$ . Final time is  $T = 1$

	$P^1$	$P^2$	$P^3$	$P^4$
$N = 10$	3.7756 1.698853 sec	4.49e-02 0.461316 sec	2.25e-03 1.484495 sec	1.58e-04 3.264180 sec
$N = 20$	1.0142 1.970224 sec	4.12e-03 7.825409 sec	1.43e-04 22.669124 sec	5.97e-06 61.202388 sec
$N = 30$	4.56e-01 10.394017 sec	1.14e-03 45.629297 sec	2.84e-05 148.329982 sec	
$N = 40$	2.57e-01 47.897740 sec	4.16e-04 229.812872 sec	9.31e-06 858.087922 sec	

Table 4: Errors for Example 1 when using  $P^k$ ,  $k = 1, 3, 4$  polynomials on a uniform mesh of  $N \times N$  cells,  $\beta = 10$ . Final time is  $T = 1$

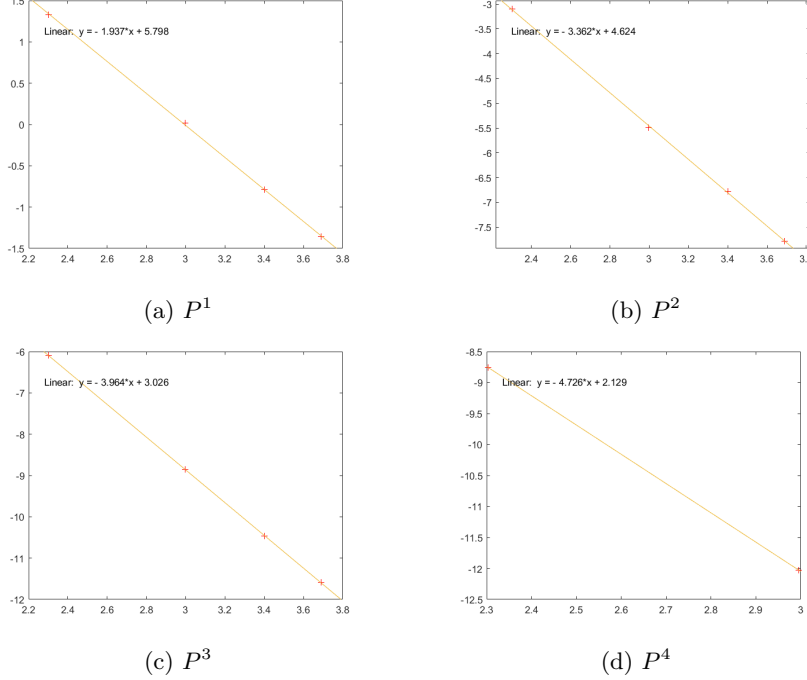


Figure 13: Order of errors for Table 4

	$P^1$	$P^2$	$P^3$	$P^4$
$N = 10$	5.5707 0.356271 sec	5.70e-02 0.551440 sec	2.32e-03 1.628625 sec	2.00e-04 3.440824 sec
$N = 20$	1.5194 2.063547 sec	4.6e-03 8.175631 sec	1.50e-04 25.686445 sec	7.71e-06 59.034659 sec
$N = 30$	6.83e-01 9.972972 sec	1.12e-03 47.501327 sec	3.28e-05 207.465674 sec	
$N = 40$	3.86e-01 34.040576 sec	4.66e-04 190.805088 sec	1.02e-05 672.644482 sec	

Table 5: Errors for Example 1 when using  $P^k$ ,  $k = 1, 3, 4$  polynomials on a uniform mesh of  $N \times N$  cells,  $\beta = 15$ . Final time is  $T = 1$

*Example 2:* We take the nonlinear Schrödinger equation

$$iu_t + \Delta u + 2|u|^2 u = 0, \quad u(x, y, 0) = \sqrt{2}e^{i(x+y)}, \quad (x, y) \in [0, 2\pi]^2, \quad t \geq 0,$$

with periodic boundary condition which has the exact solution

$$u(x, y, t) = \sqrt{2}e^{i(x+y+2t)}.$$

In this example, we take the flux parameter  $\beta = 0$ , and use polynomial  $P^k$  for  $k = 1, 2, 3, 4$  on uniform mesh with  $N \times N$  rectangular cells where  $N = 10, 20, 40$ . For time steps  $\Delta t = 0.002$ , we have the Table 6 for the errors and Figure 14 for the order of errors. The blank parts in the table are due to computational limitations of the computer that is used for solving the problem.

	$P^1$	$P^2$	$P^3$	$P^4$
$N = 10$	4.11e-01	1.22e-01	1.14e-02	5.88e-04
$N = 20$	9.17e-02	1.88e-02	4.05e-04	2.81e-05
$N = 40$	2.20e-02	7.93e-04		

Table 6: Errors for Example 2 when using  $P^k$ ,  $k = 1, 3, 4$  polynomials on a uniform mesh of  $N \times N$  cells,  $\beta = 0$ . Final time is  $T = 1$

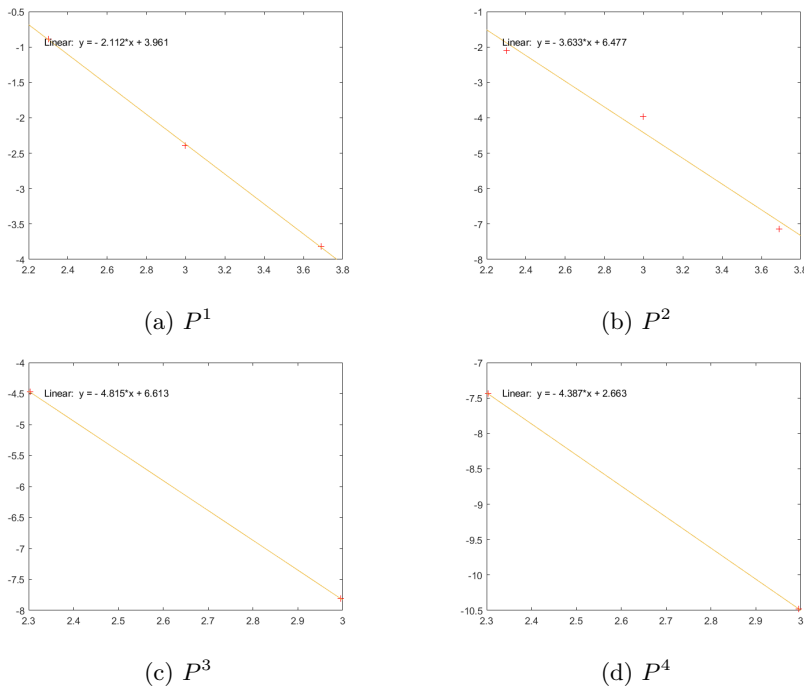


Figure 14: Order of errors for Table 6

## 4 Discussion and Conclusion

In this study, we have used discontinuous Galerkin method to solve both linear and nonlinear Schrödinger equations with periodic boundary conditions in one dimensional and two dimensional cases. For time discretization, we used a third order Runge-Kutta method for the nonlinear one dimensional case, Crank-Nicolson for the linear two dimensional case and Strang Splitting for the nonlinear two dimensional case. In our numerical examples, we use uniform mesh with regular polynomial space. Our results confirm the reliability and power of discontinuous Galerkin method. Our results show that Discontinuous Galerkin method have optimal order of accuracy  $O(h^{k+1})$  where  $h$  is the mesh spacing and  $k$  is the degree of the polynomial expansion used. The numerical tests show accuracy and efficiency of the Discontinuous Galerkin method.

## References

- [1] H. Liu, Y. Huang, W. Lu, N. Yi, On accuracy of the mass-preserving DG method to multi-dimensional Schrödinger equations. *IMA Journal of Numerical Analysis*, Volume 39, Issue 2, April 2019, Pages 760–791
- [2] L. Kong, J. Hong, L. Ji, P. Zhu, Compact and efficient conservative schemes for coupled nonlinear Schrödinger equations. *Numerical Methods for Partial Differential Equations*, 31(6), pp.1814-1843. 2015
- [3] C.-W. Shu. Discontinuous Galerkin methods for time-dependent convection dominated problems: Basics, recent developments and comparison with other methods. In Building Bridges: *Connections and Challenges in Modern Approaches to Numerical Partial Differential Equations*, pages 369-397. Springer, 2016.
- [4] Y. Cheng, C.-S. Chou, F. Li, and Y. Xin, L<sub>2</sub> stable discontinuous Galerkin methods for one-dimensional two-way wave equations. *Mathematics of Computation*, 86(303):121-155, 2017.
- [5] A. Chen, F. Li, Y. Cheng, An ultra-weak discontinuous Galerkin method for Schrödinger equation in one dimension. *Journey of Scientific Computing* Volume 78, 2019, Pages 772-815.
- [6] W. Lu, Y. Huang, and H. Liu. Mass preserving discontinuous Galerkin methods for Schrödinger equations. *Journal of Computational Physics*, 282:210-226, 2015.
- [7] U. M. Ascher, S. J. Ruuth, and R. J. Spiteri. Implicit-explicit Runge-Kutta methods for time-dependent partial differential equations. *Applied Numerical Mathematics*, 25(2-3):151-167, 1997.
- [8] B. Cockburn and C.-W. Shu. The local discontinuous Galerkin method for time-dependent convection-diffusion systems. *SIAM Journal on Numerical Analysis*, 35(6):2440-2463, 1998.
- [9] B. Cockburn and C.-W. Shu. TVB Runge-Kutta local projection discontinuous Galerkin finite element method for conservation laws. ii. general framework. *Mathematics of computation*, 52(186):411-435, 1989.
- [10] B. Cockburn, S.-Y. Lin, and C.-W. Shu. TVB Runge-Kutta local projection discontinuous Galerkin finite element method for conservation laws iii: one-dimensional systems. *Journal of Computational Physics*, 84(1):90-113, 1989.
- [11] B. Cockburn, S. Hou, and C.-W. Shu. The Runge-Kutta local projection discontinuous Galerkin finite element method for conservation laws. iv. the multidimensional case. *Mathematics of Computation*, 54(190):545-581, 1990.
- [12] B. Cockburn and C.-W. Shu. The Runge-Kutta discontinuous Galerkin method for conservation laws v: multidimensional systems. *Journal of Computational Physics*, 141(2):199-224, 1998.

- [13] X. Liang, A. Q. M. Khaliq, and Y. Xing. Fourth order exponential time differencing method with local discontinuous Galerkin approximation for coupled nonlinear Schrödinger equations. *Communications in Computational Physics*, 17(2):510-541, 2015.
- [14] E. Hairer and G. Wanner, Solving Ordinary Differential Equations II: Stiff and Differential-Algebraic Problems (Springer, New York, 1991).
- [15] Lu, W.Y., Huang, Y. Q. and Liu, H. (2015) Mass preserving direct discontinuous Galerkin methods for Schrödinger equations. *J. Comp. Phys.*, 282, 210–226.
- [16] W. Reed and T. Hill. Triangular mesh methods for the neutron transport equation. La-ur-73-479, Los Alamos Scientific Laboratory, 1973.
- [17] G. Jiang and C.-W. Shu. On a cell entropy inequality for discontinuous Galerkin methods. *Math. Comp.*, 62:531-538, 1994.
- [18] Kirby, R.M., Karniadakis, G.E. Selecting the Numerical Flux in Discontinuous Galerkin Methods for Diffusion Problems. *J Sci Comput* 22, 385–411 (2005)
- [19] M. Zhang and Chi-Wang Shu, An Analysis of Three Different Formulations of the Discontinuous Galerkin Method for Diffusion Equations, 2002